Macromolecules
ARTICLE

Macromolecules **2010**, *43*, 6361–6367 **6361**
DOI: 10.1021/ma1001639

Anthradithiophene-Containing Copolymers for Thin-Film Transistors and Photovoltaic Cells

Ying Jiang,[†] Toshihiro Okamoto,[†] Hector A. Becerril,[†] Sanghyun Hong,[†] Ming Lee Tang,[‡] Alex C. Mayer,[§] Jack E. Parmer,[§] Michael D. McGehee,[§] and Zhenan Bao*,[†]

[†]*Department of Chemical Engineering, Stanford University, Stanford, California 94305-5025,*
[‡]*Department of Chemistry, Stanford University, Stanford, California 94305-5080, and*
[§]*Department of Material Science and Engineering, Stanford University, Stanford, California 94305-4034*

Received January 23, 2010; Revised Manuscript Received June 25, 2010

ABSTRACT: We synthesized anthradithiophene−cyclopentadithiophene conjugated copolymers via Stille coupling. The anthradithiophene core was verified to be superior in stability compared to pentacene toward Diels−Alder cycloaddition and therefore more compatible with fullerenes, acceptor material commonly used in bulk heterojunction (BHJ) photovoltaic cells. The polymers exhibit high film absorption coefficients of 10^5 cm^{-1}, an order of magnitude higher than previously reported anthradithiophene−dialkylfluorene copolymers. Short-circuit currents exceeding 5 mA/cm^2 and a BHJ device efficiency close to 1% were achieved when device morphology was improved with diiodooctane as a solvent additive. This is the highest power conversion efficiency achieved by an acene-containing polymer so far.

Introduction

Conjugated polymers with semiconducting properties hold promise for lowering the cost of large area optoelectronic applications. This has become more evident in the past decade when these polymers are fast realizing their potential as active materials in optoelectronic device applications. As a prime example, derivatives of regioregular polythiophene have been extensively investigated as candidates for organic field-effect transistor (OFET)[1−4]and organic photovoltaic (OPV)[5] applications. In addition, copolymers of carbazole[6,7] and various other donor−acceptor types of conjugated polymers[8−14] have also contributed remarkably in their performance in the field of OPVs.

We previously reported an emerging class of polymers based on the incorporation of five-fused-ring acene moieties. Specifically, alternating triisopropylsilylethynyl-substituted pentacene (TIPSEP) and anthradithiophene (TIPSEADT) containing copolymers were synthesized using Sonogashira and Suzuki coupling reactions.[15,16] While pentacene is a small molecule with exemplary electronic properties, achieving field-effect mobilities surpassing those of amorphous silicon,[17−22] it also has a favorable absorption range in thin-film for OPV application, achieving power conversion efficiencies (PCEs) exceeding 2% in a bilayer heterojunction configuration with C_{60}.[23−25] Building an acene-containing conjugated polymer potentially allows one to utilize the superior charge-transport properties resulting from a likely π-stack of large fused aromatic systems and, at the same time, benefit from the solution processability of a polymer.

The anthradithiophene (ADT) unit has been of interest because its charge-transport properties are comparable to those of pentacene,[21,26,27] while its absorption range in thin film (2.2 eV)[16] is reasonably broad. Alkyl-functionalized triethylsilylethynyl-ADT has shown promising photovoltaic properties in a bulk heterojunction with phenyl-C_{61}-butyric acid methyl ester ($PC_{61}BM$), achieving power conversion efficiency of over 2%.[28] Another important advantage of ADT is that it is more stable than pentacene toward oxidation.[26] In addition, for a bulk heterojunction photovoltaic cell architecture, whose active layer is usually spin-cast from a homogeneous mixture of the donor polymer and the acceptor (usually $PC_{61}BM$), chemical stability of the polymer with respect to the acceptor $PC_{61}BM$ is of foremost importance.

In this work, we experimentally compared and verified the superior stability of TIPSEADT compared to TIPSEP with $PC_{61}BM$ in the mixture. We also report a new molecular design following that of the TIPSEADT−fluorene copolymer, employing cyclopentadithiophene as a donor moiety. Knowing that adjacent thiophene units have a smaller torsional angle as compared to adjacent thiophene and phenyl units, we sought to synthesize a more coplanar ADT-containing polymer structure to enhance absorption strength, a property related to the planarity of the conjugated backbone. The TIPSEADT−fluorene and TIPSEADT−cyclopentadithiophene copolymers were functionalized with *n*-octyl and 2-ethylhexyl side chains at the C9 and C4 positions of fluorene and cyclopentadithiophene (CPDT), respectively. Linear and branched side chains were chosen to investigate potential packing properties of the polymers, which impact electronic device performances, as observed in the literature.[10] The field-effect transistor and photovoltaic cell properties of the four polymers are investigated and compared. In particular, our study reveals the impact of molecular weight and film morphology on the photovoltaic performance of the TIPSEADT−CPDT copolymer with linear side chain.

Experimental Section

The synthesis of TIPSEADT-containing copolymers is summarized in Scheme 1. Solvents and chemicals were purchased from Sigma-Aldrich Co. and used as received unless otherwise stated. The synthesis of 5,11-bis(triisopropylsilylethynyl)dibromoanthradithiophenes (TIPSE-Br_2-ADT) (as a mixture of syn and anti isomers) was carried out according to previous literature procedures.[16] **P1a** and **P1b** were synthesized using previously reported Suzuki coupling method[16] in 92% and 93% yield, respectively. **P2a** and **P2b** were synthesized with Stille coupling

*Corresponding author. E-mail: zbao@stanford.edu.

Published on Web 07/12/2010

Scheme 1. Synthesis of P1a, P1b from Suzuki Coupling and P2a, P2b from Stille Coupling[a]

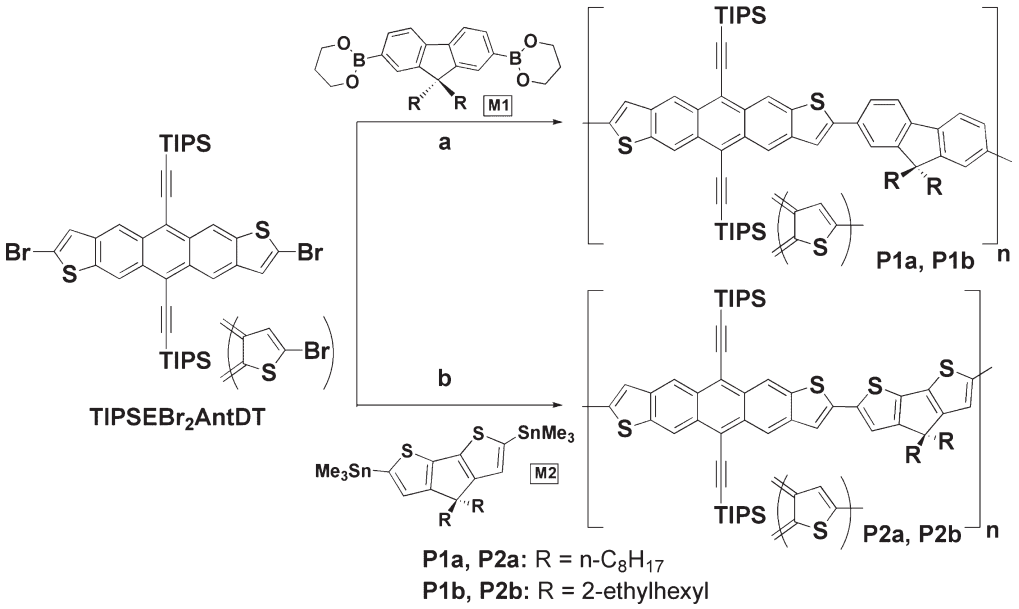

[a] Reagents and conditions: (a) $Pd(PPh_3)_4$, K_2CO_3, Aliquat 336, toluene, 90 °C, 72 h; (b) $Pd_2(dba)_3$, $(o\text{-Tol})_3P$, chlorobenzene, 82 °C, 24−72 h.

Table 1. Electrochemical and Photophysical Properties of Polymers P1a, P1b, P2a, and P2b

			in *o*-DCB	in thin film	
polymers	M_n[a] (g/mol)	PDI[a]	optical E_g[b] (eV)	E_{onset}[c] (eV)	optical E_g[d] (eV)
P1a	21620	1.59	2.03	5.22	1.82
P1b	9400	1.71	2.05	5.21	2.04
P2a	12500	2.0	1.81	5.14	1.72
P2a-L	8900	2.0	1.81	5.14	1.72
P2b	28360	1.19	1.86	5.16	1.79

[a] Determined from GPC using the THF soluble part using polystyrene as a standard and THF as an eluent. [b] Estimated from the onset of absorption of solutions in *o*-DCB. [c] HOMO estimated from the ionization potential measured with photoelectron spectroscopy. [d] Estimated from the onset of absorption of thin films.

between TIPSE-Br_2-ADT and the bis(trimethylstannyl)cyclopentadithiophene (CPDT) in 68% and 89% yield, respectively, after all purification steps. **P2a** was also prepared using microwave-assisted Stille coupling reaction using a CEM Discover microwave reactor. The procedure yielded a copolymer with lower molecular weight, which is subsequently named as **P2a-L**. The difference in the batch properties was later used as an additional parameter in assessing the copolymer's photovoltaic device performance. The molecular weights and polydispersity indices of the polymers, as summarized in Table 1, were determined by gel permeation chromatography (GPC) with tetrahydrofuran (THF) as an eluent and polystyrene as a standard.

General Synthesis Procedures for TIPSEADT-*alt*-F Polymers (P1a, P1b). TIPSEADT-*alt*-F polymers were synthesized[16] with 9,9-dialkylfluorene-2,7-diboronic acid bis(1,3-propanediol) ester (**M1**) from Aldrich. The resulting polymers were washed with acetone followed by hexane in a Soxhlet setup under argon for 24 h.

P1a was previously reported in the literature.

P1a. ^{1}H NMR (400 MHz, $CDCl_3$): δ 9.22−9.02 (br), 7.98−7.66 (br), 2.35−1.83 (br), 1.50−1.00 (br), 0.85−0.70 (br). Anal. Calcd for $(C_{69}H_{90}S_2Si_2)_n$: C, 79.71; H, 8.72. Found: C, 77.39; H, 8.98.

P1b. ^{1}H NMR (500 MHz, $CDCl_3$): δ 9.24−9.06 (br), 8.04−7.58 (br), 2.35−1.90 (br), 1.50−1.16 (br), 1.06−0.50 (br). Anal. Calcd for $(C_{69}H_{90}S_2Si_2)_n$: C, 79.71; H, 8.72. Found: C, 75.80; H, 8.45.

General Synthesis Procedures for TIPSEADT-*alt*-CPDT Polymers (P2a, P2b). A dry, nitrogen-flushed Schlenk tube was charged with 4,4-bis(2-ethylhexyl)-2,6-bis(trimethylstannyl)-4*H*-cyclopenta-[2,1-*b*:3,4-*b*′]dithiophene (**M2**)[29] (107.3 mg, 1.0 mol amt), TIPSE-Br_2-ADT (1.0 mol amt), $Pd_2(dba)_3$ (0.03 mol amt), $(o\text{-Tol})_3P$ (0.3 mol amt), and chlorobenzene (0.04 M based on TIPSE-Br_2-ADT). The mixture was degassed three times using the freeze−pump−thaw method and then heated to 80−85 °C for 24−72 h. The mixture was then poured into a mixture of methanol and hydrochloric acid. The precipitate was filtered and thoroughly washed with methanol, acetone, and hexanes and extracted with hot chloroform overnight under argon in a Soxhlet setup. The polymer solution was stirred with a metal scavenger[30] at room temperature for 2 h in an inert atmosphere and then filtered through a 0.45 μm pore size PTFE syringe filter. Final precipitation in methanol, filtration, and drying afforded the desired polymer.

Microwave Synthesis Procedures for P2a-L. An oven-dried microwave tube was charged in air with **M2** (132.9 mg, 1.0 mol amt), TIPSE-Br_2-ADT (1.0 mol amt), $Pd_2(dba)_3$ (0.03 mol amt), $(o\text{-Tol})_3P$ (0.3 mol amt), and toluene (0.04 M based on TIPSE-Br_2-ADT). The tube was sealed and the mixture purged with argon for an hour. The tube was then heated in a microwave reactor for 1 h at 300 W power. The resulting polymer mixture is precipitated in a mixture of methanol and hydrochloric acid and subsequently purified in the same manner as **P2a** was.

P2a. ^{1}H NMR (500 MHz, $CDCl_3$): δ 9.25−8.75 (br), 7.52−7.35 (br), 7.10−6.85 (br), 2.00−0.60 (br). Anal. Calcd for $(C_{65}H_{86}S_4Si_2)_n$: C, 74.22; H, 8.24. Found: C, 74.34; H, 8.45.

P2b. ^{1}H NMR (500 MHz, $CDCl_3$): δ 9.25−8.75 (br), 7.52−7.35 (br), 7.10−6.85 (br), 2.00−0.60 (br). Anal. Calcd for $(C_{65}H_{86}S_4Si_2)_n$: C, 74.22; H, 8.24. Found: C, 73.27; H, 7.95.

Stability Analysis. 4 mg of TIPSE-Br_2-P or TIPSE-Br_2-ADT and $PC_{61}BM$ were added to an NMR tube and were dissolved in anhydrous, oxygen-free d_6-benzene in a nitrogen atmosphere to form a homogeneous mixture. The mixture was monitored with nuclear magnetic resonance (NMR) spectroscopy for 24 h.

Electrochemical and Photophysical Properties Measurement. Cyclic voltammetry (CV) experiments were performed under a stream of argon in anhydrous *o*-DCB with 0.05 M tetra-*n*-butylammonium hexafluorophosphate (^{n}Bu$_4$NPF$_6$) as a supporting electrolyte. Platinum electrodes were used at a scan rate of 100 mV s^{-1} with the Fc/Fc^+ redox system as an internal reference oxidation potential for both polymers **P1a** and **P1b**.

Films for UV−vis were prepared by spin-casting 5 mg/mL polymer solutions from chloroform (at 800 rpm). Their thicknesses were measured on a Dektak 150 profilometer (Veeco Metrology Group). Films drop-cast from 1 mg/mL polymer solutions in chloroform were used for the measurement of onset ionization energy in a Riken AC-2 spectrometer. Photoluminescence spectra were recorded on an Horiba Jobin Yvon FL3-2IHR fluorometer.

OTFT Fabrication and Measurement. Active organic semiconductor layers were deposited on octadecyltrichlorosilane (OTS)-modified SiO_2/Si substrates by drop-casting from 1 mg/mL polymer solutions in *o*-DCB at 110 °C. Typical drying times were 25 min. Residual solvent removal and film annealing were carried out at 170 °C for 1 h. 40 nm thick gold electrodes were deposited on the polymer films through a shadow mask. $I-V$ characterization was carried out using a Keithley 4200, four-channel semiconductor parametric analyzer with femtoamp resolution. All devices were electrically tested inside a nitrogen glovebox.

Solar Cell Fabrication, Measurement, and Characterization. Indium tin oxide (ITO) on glass was cleaned and deposited with a 30 nm thick poly(3,4-ethylenedioxythiophene)poly(styrenesulfonate) (PEDOT:PSS) layer of resistivity 1 kΩ·cm. The polymers were dissolved in *o*-DCB overnight at 60 °C. PCBM was then blended with the polymer solution for 3 h at 95 °C. The hot blend was immediately spin-cast on ITO at 400−700 rpm over 70 s. The resulting films were allowed to dry and solvent anneal overnight in a covered Petri dish under room temperature, before depositing 100 nm thick aluminum electrodes through a shadow mask. The active layer thicknesses of the solar cells is typically 110 nm. $I-V$ characterization was carried out in the dark and under simulated 1 sun AM 1.5 radiation with a Keithly 2400 source meter. Illumination was achieved with a 91160 300 W Oriel solar simulator equipped with a 6258 ozone-free Xe lamp and an air mass AM 1.5 G filter. Tapping mode atomic force microscopy (AFM) investigation of the solar cell films was done using a Multimode Nanoscope III with Extender electronics (Veeco Metrology Group).

Results and Discussion

Reactivity of Anthracenedithiophene vs Pentacene toward $PC_{61}BM$. Higher polyacenes suffer from instability and poor solubility, posing challenges to material processing and device stability. Pentacene, for example, is known to be susceptible toward Diels−Alder cycloaddition reaction in the presence of strong dienophiles such as fullerene derivatives.[31,32] In fact, Li et al. reported the preparation of tetracene−fullerene Diels−Alder adducts as novel electron-accepting materials for a bulk heterojunction cell.[33] Thienoacenes, on the other hand, are known to be more stable compared to the analogous carbocyclic acene.[28] In view of limitations in the device performance we could achieve with pentacene-containing polymers as the active material (unpublished results), we sought to further verify the stability of TIPSE-Br_2-P and TIPSE-Br_2-ADT in solution with respect to $PC_{61}BM$ employing ^1H NMR spectroscopy in benzene-d_6. Spectra recorded for mixtures of either TIPSE-Br_2-P or TIPSE-Br_2-ADT with $PC_{61}BM$ (given in the Supporting Information) showed that, while prepared under the same inert conditions, a mixture of TIPSE-Br_2-P and $PC_{61}BM$ in benzene-d_6 reacted almost instantaneously. In comparison, a mixture of TIPSE-Br_2-ADT and $PC_{61}BM$ (Figure S1b) is stable over 7 days. While bulk heterojunction devices are typically prepared under an inert atmosphere, the result of the experiment shows that the rate of cycloaddition reaction is non-negligible on the time scale of device preparation. It can be concluded that a mixture of pentacene derivatives and $PC_{61}BM$ is not stable in the solution, and its solution-cast bulk heterojunction film contains undesired impurities. This ultimately limited the device efficiency of our pentacene copolymer BHJ devices by forming defects. In comparison, the ADT unit is better suited as an active component for bulk-heterojunction solar cells.

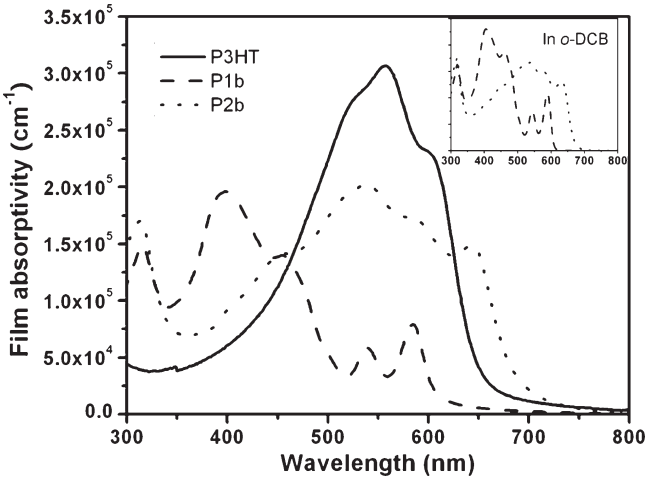

Figure 1. Film absorption coefficients of P3HT, **P1b**, and **P2b** (inset shows the copolymers' absorption in *o*-DCB).

Electrochemical and Photophysical Properties of TIPSE-ADT Copolymers. The highest-occupied molecular orbital (HOMO) and lowest-unoccupied molecular orbital (LUMO) energy levels, as well as the optical bandgaps, were determined using UV−vis absorption spectroscopy and photoelectron spectroscopy (PES) for the polymers in both solution and thin-film states. A summary of the photophysical and electrochemical properties is given in Table 1.

The onsets of ionization of the thin films as measured by photoelectron spectroscopy show that **P2a** and **P2b** have shallower frontier orbital energy levels (∼5.15 eV) than those of the fluorene copolymers **P1a** and **P1b** (∼5.20 eV). The absorption onset of the **P2a** and **P2b** copolymers of around 670 nm, too, precedes that of **P1a** and **P1b** by about 60 nm (Figure 1). The red shift in absorption arose from the increase in planarity between the thiophene moieties on ADT and CPDT comonomers in the absence of steric hindrance from the phenyl hydrogens, leading to better overlap between the frontier orbitals and a lower bandgap. Cyclopentadithiophene being the donor moiety also enhanced the thin-film absorption coefficient of **P2a** and **P2b** by an order of magnitude as compared to **P1a** and **P1b** (Figure 2). It is clear that the former are able to achieve the same order of magnitude in absorptivity (of 10^5 cm^{-1}) as the highly absorbing poly(3-hexylthiophene) (P3HT).

Field-Effect Transistor Performance. The materials were evaluated for their performance in field-effect transistor devices. Their performance is summarized in the Supporting Information (Table S1). Devices annealed at 170 °C prior to electrode deposition showed field-effect mobilities on the order of 10^{-3} $cm^2/(V\ s)$ and higher. Devices fabricated with **P1a** as the active layer were able to achieve close to 0.01 $cm^2/(V\ s)$ in hole mobility. The current−voltage relations of **P1a** and **P2a** devices are illustrated in Figure 2. Comparing the output characteristics, we observe that the saturation output current of **P2a** at 100 V gate bias is higher than that of **P1a** (while the transfer characteristics yielded a higher hole mobility for **P1a** as compared to **P2a**). This observation could be due to contact resistances arising from specific morphological imperfections at the metal−polymer interface. Further transistor device fabrication and analysis may

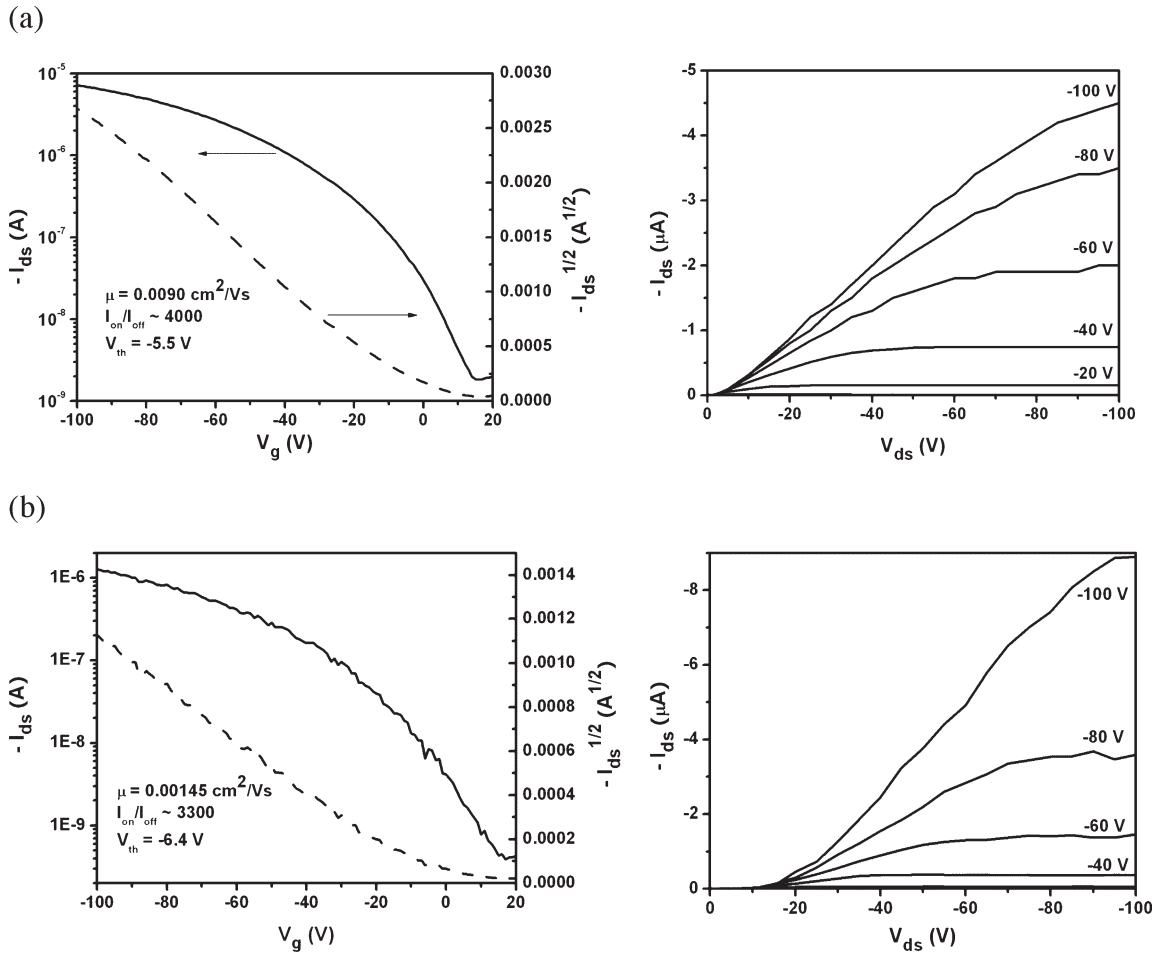

Figure 2. Representative $I-V$ (at $V_{ds} = -100$ V) and output characteristics of p-type OTFT devices of (a) **P1a** and (b) **P2a**.

extract contact-effect-free device characteristics for these materials[34] and could be part of future studies to increase understanding of these systems.

While we anticipated different film morphology and device characteristics for polymers with linear or branched side chains, as it was the case observed for several classes of polymers,[10] we did not observe any overall appreciable differences between the transistor performances of the fluorene and cyclopentadithiophene copolymers with different side chains over the devices we measured. The reason that **P1a** yielded devices with hole mobility of 9×10^{-3} cm^2/(V s), a factor of 7−8 higher than those of the rest ($(1.2-1.5) \times 10^{-3}$ cm^2/(V s)), could not be discerned from examining the morphology and presence of crystallinity of the polymer films, for both polymers with linear and branched alkyl side chains were verified to be amorphous by grazing-incidence X-ray diffraction (GIXD) and differential scanning calorimetry (DSC). Processing conditions could have resulted in different film morphologies that impact charge transport.

Considering these polymers are generally amorphous, it is to be noted that their FET mobilities, on the order of 10^{-3} cm^2/(V s), are relatively high.[35,36] Furthermore, even though FET mobilities are not a direct indication of charge transport properties of the neat materials in a BHJ solar cell blend, they have been found to provide a good correlation with diode mobility measured for thin films.

Photovoltaic Properties. The photovoltaic properties of the copolymers, including **P2a** with different molecular weights, were investigated, and the results are summarized in Table 2a. In our previous communication,[16] polymer **P1a** was preliminarily evaluated for photovoltaic performance and achieved a power conversion efficiency of 0.68%, with a short-circuit current (J_{sc}), open-circuit voltage (V_{oc}), and a fill factor (FF) of 2.35 mA/cm^2, 0.75 V, and 0.385, respectively. In this study, blend ratio optimization studies were carried out for **P1a** as well as **P1b**. The solar cell performance was optimized in *o*-DCB, at a polymer:$PC_{61}BM$ weight ratio of 1:4. We observed that the J_{sc} of these solar cell devices remained around 2 mA/cm^2. The cells of **P1b** had higher V_{oc} and FFs but lower currents, achieving a slightly lower but comparable efficiency of 0.57%.

Preliminary device performance of the CPDT copolymers showed a trend of higher currents and lower V_{oc} as compared to those of the fluorene copolymers. These observations could be explained by the facts that the CPDT copolymers have higher absorptivity and a larger absorption range, therefore increasing the absorption efficiency; the deeper HOMO levels of the fluorene copolymers, on the other hand, yield higher V_{oc}s, which are determined by the difference between the HOMO level of the donor polymer and the LUMO level of the acceptor.

The blend ratio optimized at between 2 times and 4 times $PC_{61}BM$, where **P2a** and **P2b** were able to achieve PCEs of 0.9% and 0.75%, respectively. **P2a-L**, in comparison, did not achieve the efficiency of the **P2a** devices under the same fabrication conditions. In particular, **P2a** was able to achieve higher currents. On average, devices made with **P2a** showed average J_{sc}s from 3.1 to 3.7 mA/cm^2, and average PCEs from 0.75% to 0.78%, as compared to 2.1 mA/cm^2 and 0.44% for **P2a-L** at the same blend ratio (Table S2 summarizes the

Table 2. Summary of Photovoltaic Properties of P1a, P1b, P2a, and P2b

(a) Blend Ratio Optimization

polymer	optimal blend ratios (with $PC_{61}BM$)	J_{sc} (mA cm^{-2})	V_{oc} (V)	FF	PCE (%)
P1a	1:3	2.35	0.75	0.39	0.68
P1b	1:4	1.31	0.965	0.45	0.57
P2a	1:2	4.20	0.675	0.32	0.91
P2a-L	1:2	2.30	0.675	0.34	0.53
P2b	1:4	2.30	0.705	0.46	0.75

(b) Optimizing **P2a-L** (M_n = 8900, PDI = 2.0) Bulk Heterojunction Cell Morphology, at a 1:2 Blend Ratio

acceptor	diiodooctane	J_{sc} (mA cm^{-2})	V_{oc} (V)	FF	PCE (%)
$PC_{61}BM$	none	2.30	0.675	0.34	0.53
$PC_{61}BM$	3 vol %	4.32	0.645	0.29	0.81
$PC_{71}BM$	3 vol %	5.26	0.615	0.29	0.94

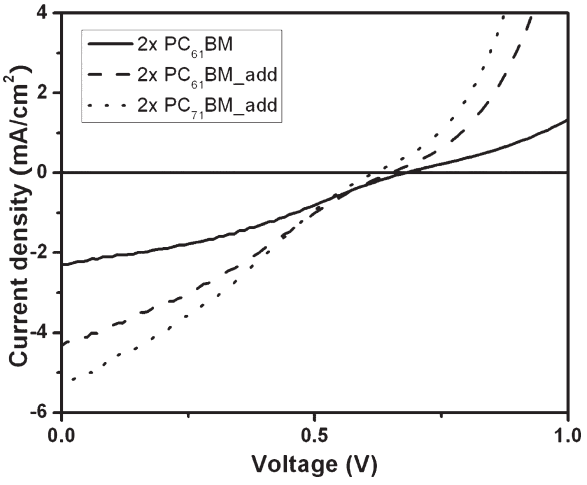

Figure 3. Improvement of current for **P2a** upon optimization, corresponding to the last three entries in Table 2.

statistical device properties). An origin of the differing device performance could be the aforementioned difference in molecular weights between **P2a** and **P2a-L**. Molecular weight is known to impact morphology and solar cell performance, with polymers of higher molecular weights yielding higher J_{sc}s, as it has been systematically shown in the literature.[37]

To investigate if the performance of **P2a-L** could be further improved by controlling film morphology (vide infra), we carried out experiments adding 3 vol % of diiodooctane to the blend. Diiodooctane, a high boiling component of the blend, has been reported to ameliorate phase segregation, and therefore J_{sc}, by selectively dissolving the fullerenes and delaying their crystallization.[38] The performance of the resulting devices of **P2a-L** is summarized in Table 2b, and the corresponding $I-V$ relationships are illustrated in Figure 3. As compared to the control devices of **P2a-L**, the devices processed with diiodooctane showed almost twice as much current. Substitution of $PC_{61}BM$ with phenyl-C_{71}-butyric acid methyl ester ($PC_{71}BM$) as the acceptor further raised J_{sc} to as high as 5.3 mA/cm^2. The V_{oc}, on the other hand, decreased by about 30 mV with $PC_{71}BM$. Despite its LUMO level being a few tens of milielectronvolts closer to vacuum than $PC_{61}BM$,[39] it is likely that a nonoptimal morphology, which slightly increased charge recombination rates, plays a more important role in dictating the V_{oc} than the theoretical linear correlation between V_{oc} and the acceptor's electron affinity. With V_{oc} and FF being

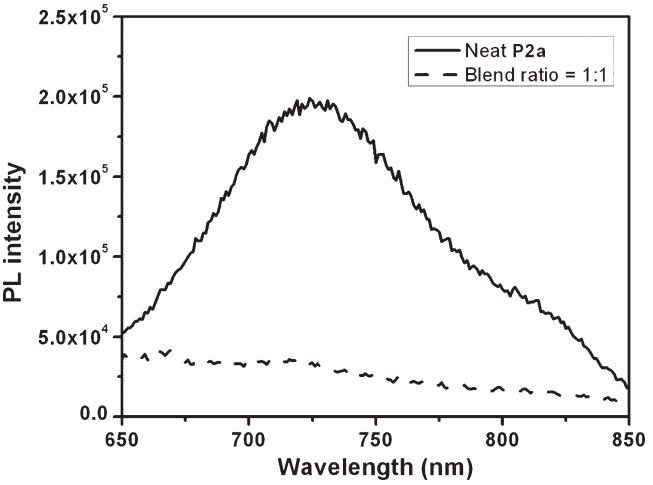

Figure 4. Photoluminescence of **P2a** neat and blended with $PC_{61}BM$ at a 1:1 ratio.

0.62 V and 0.29, the device achieved 0.93% efficiency. The external quantum efficiency of the cell corresponds well to the absorption profile of the active polymers, peaking at around 30% at 550 nm (see Supporting Information). This is the highest power conversion efficiency achieved by an acene-containing polymer. Moreover, it is to be noted that further improvements of molecular weights are anticipated to achieve improvements in morphology and device performance.

On the other hand, the devices represented in Figure 3 exhibited low fill factors. The relatively thick active layers (> 100 nm) processed from 10 mg/mL polymer solutions resulted in large series resistances on the order of 50 MΩ/cm^2. Thinner devices processed from less concentrated polymer solutions exhibited higher fill factors, but the photocurrents are limited by absorption (Table S3). Low shunt resistances of 70−100 MΩ/cm^2 are a result of rough films and subsequent current leakages. We anticipate that further process condition optimization to enhance electrical contacts would improve the performance of bulk heterojunction cells fabricated from the ADT−CPDT copolymers.

Photoluminescence Quenching and Thin Film Morphology. Photoluminescence quenching experiments and atomic force microscopy (AFM) were carried out to further understand the impact of blend ratio and solvent additive on device performance. Photoluminescence quenching studies of **P2a** blend films, fabricated under the same conditions as those for the bulk heterojunction devices, show that a blend ratio of 1:1 is sufficient to quench all of the polymer's luminescence (Figure 4). On the other hand, blend ratios closer to 1:4 typically yield devices with higher fill factors (Table S3). Combined, these observations suggest that the quantum efficiency at lower blend ratios was limited less by the exciton splitting process than by factors that impacted charge collection efficiency. One such factor, for example, could originate from Mayer et al.'s model of intercalating fullerenes between sufficiently widely spaced side chains of donor polymers, which explains the need for a higher blend ratio to form a continuous electron-transporting phase.[40] At such ratios, with a higher proportion of the less absorbing PCBM, the **P2a** devices become limited in absorption and hence short-circuit current (Table S3). An intermediate blend ratio compromising current and fill factor yielded the optimal performance for the polymer.

Examining the morphologies of the blend films of **P2a** using AFM, it can be observed that the blend ratio of 1:1

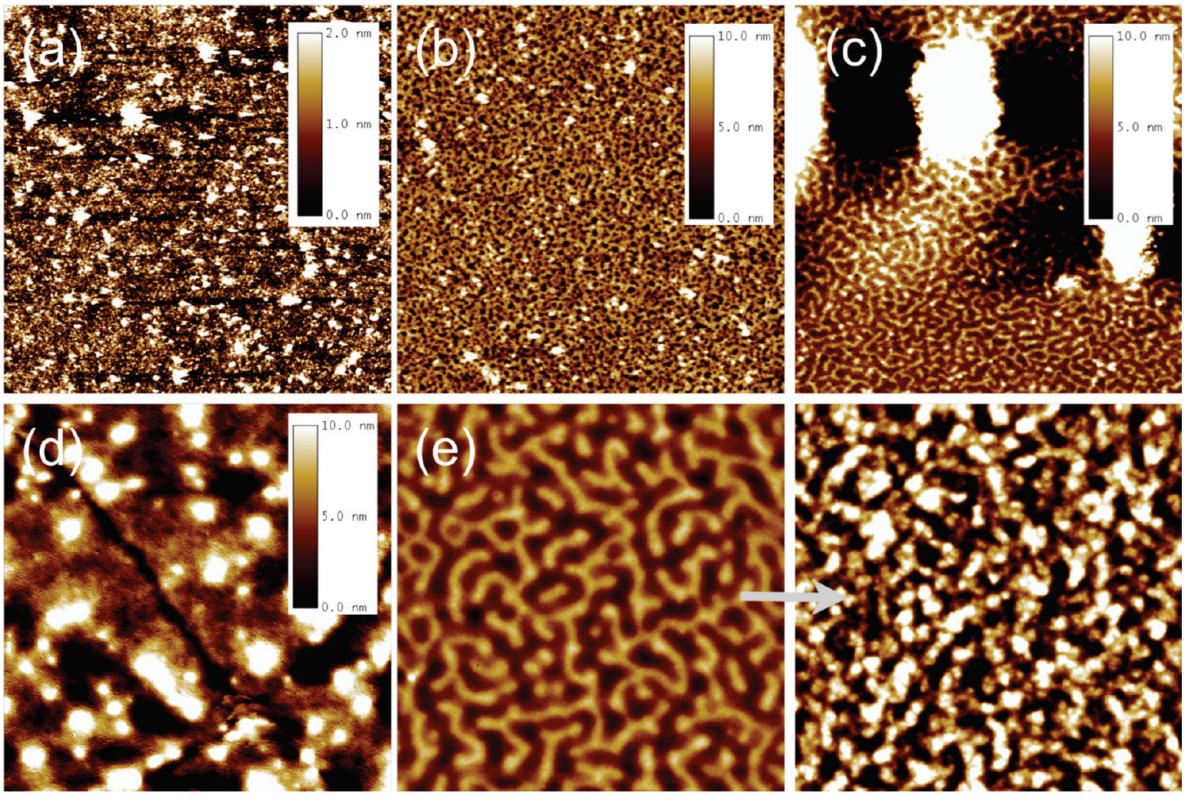

Figure 5. Tapping-mode AFM height images (5 μm × 5 μm) of (a) neat **P2a** and **P2a**/PCBM blend films with blend ratios of (b) 1:1, (c) 1:2, and (d) 1:4. (e) AFM height images (1 μm × 1 μm) shows the transformation of morphology (from the left panel to the right) when 3 vol % diiodooctane was used as a solvent additive, at a 1:2 blend ratio.

generated isolated domains (Figure 5b) as compared to a much smoother film of neat polymer (Figure 5a). The domains are on the order of 100 nm in size; they clearly become more interconnected as the blend ratio increased (Figure 5c) and become very much less defined as the blend ratio was increased to 1:4 (Figure 5d). While the interconnection of the domains may not directly suggest a development of a bicontinuous morphology on the much smaller scale of molecular mixing, it could be linked to the improvement in the fill factors at higher blend ratios, implying improved charge collection efficiencies.

More interestingly, AFM verifies that the morphology of **P2a-L** films at 1:2 blend ratio processed with or without diiodooctane are significantly different (Figure 5e). The clear-cut distinction between the two phases disappeared for blends processed with the additive, resulting in a more homogeneous film topography. The fact that photocurrents extracted were nearly twice as high suggests that this is a more optimal morphology, possibility facilitating charge transport.

Conclusion

We have synthesized anthradithiophene-containing copolymers with fluorene and CPDT as comonomers using Suzuki and Stille coupling reactions. The CPDT-containing copolymers showed better photovoltaic performance owing to their higher absorption in thin film, giving rise to high short-circuit currents; on the other hand, they gave lower open-circuit voltages than the fluorene-containing copolymers due to higher-lying HOMO energy levels. By incorporating diiodooctane while processing the devices, the film morphology was improved and **P2a** (ADT-C_8-CPDT) was able to achieve a power conversion efficiency of close to 1%. While the device performance fell short of the promises the copolymers hold, improvements in molecular weights, solubility, and purity will potentially yield better performance. Additional device optimization procedures such as the modification of electrode contact and tuning of morphology could potentially eliminate parasitic external resistances and improve the devices' fill factors. Further studies on the bulk heterojunction systems based on these materials are warranted.

Acknowledgment. Z.B. acknowledges financial support from the Stanford Global Climate and Energy Project and the Air Force Office of Scientific Research. This publication was also partially based on work supported by the Center for Advanced Molecular Photovoltaics (Award No. KUS-C1-015-21), made by King Abdullah University of Science and Technology (KAUST). Y.J. acknowledges financial support from the Agency of Science, Technology and Research of Singapore.

Supporting Information Available: Figures S1−S5 and Tables S1−S4. This material is available free of charge via the Internet at http://pubs.acs.org.

References and Notes

(1) Bao, Z.; Dodabalapur, A.; Lovinger, A. J. *Appl. Phys. Lett.* **1996**, *69*.
(2) Ong, B. S.; Wu, Y.; Liu, P.; Gardner, S. *J. Am. Chem. Soc.* **2004**, *126* (11), 3378–3379.
(3) McCulloch, I.; Heeney, M.; Bailey, C.; Genevicius, K.; MacDonald, I.; Shkunov, M.; Sparrowe, D.; Tierney, S.; Wagner, R.; Zhang, W.; Chabinyc, M. L.; Kline, R. J.; McGehee, M. D.; Toney, M. F. *Nature Mater.* **2006**, *5*.
(4) Bao, Z.; Locklin, J. Organic Field-Effect Transistors, 1st ed.; CRC Press: Florida, 2007.
(5) Li, G.; Shrotriya, V.; Huang, J.; Yao, Y.; Moriarty, T.; Emery, K.; Yang, Y. *Nature Mater.* **2005**, *4*, 864–868.

(6) Nicolas, B.; Alexandre, M.; Mario, L. *Adv. Mater*. **2007**, *19* (17).
(7) Park, S. H.; Roy, A.; Beaupre, S.; Cho, S.; Coates, N.; Moon, J. S.; Moses, D.; Leclerc, M.; Lee, K.; Heeger, A. J. *Nature Photonics* **2009**, *3* (5), 297–302.
(8) Becerril, H. A.; Miyaki, N.; Tang, M. L.; Mondal, R.; Sun, Y.-S.; Mayer, A. C.; Parmer, J. E.; McGehee, M. D.; Bao, Z. *J. Mater. Chem*. **2009**, *19*, 591–593.
(9) Mondal, R.; Ko, S.; Norton, J.; Miyaki, N.; Becerril, H. A.; Verploegen, E.; Toney, M. F.; Brédas, J. L.; McGehee, M. D.; Bao, Z. *J. Mater. Chem*. **2009**.
(10) Mondal, R.; Miyaki, N.; Becerril, H. A.; Norton, J. E.; Parmer, J.; Mayer, A. C.; Tang, M. L.; Brédas, J.-L.; McGehee, M. D.; Bao, Z. *Chem. Mater*. **2009**, *21* (15), 3618–3628.
(11) Hou, J.; Chen, H.-Y.; Zhang, S.; Li, G.; Yang, Y. *J. Am. Chem. Soc*. **2008**, *130* (48), 16144–16145.
(12) Peet, J.; Kim, J. Y.; Coates, N. E.; Ma, W. L.; Moses, D.; Heeger, A. J.; Bazan, G. C. *Nature Mater*. **2007**, *6* (7), 497–500.
(13) Chen, H.-Y.; Hou, J.; Zhang, S.; Liang, Y.; Yang, G.; Yang, Y.; Yu, L.; Wu, Y.; Li, G. *Nature Photonics* **2009**, *3* (11), 649–653.
(14) Cheng, Y.-J.; Yang, S.-H.; Hsu, C.-S. *Chem. Rev*. **2009**, *109* (11), 5868–5923.
(15) Okamoto, T.; Bao, Z. *J. Am. Chem. Soc*. **2007**, *129*, 10308–10309.
(16) Okamoto, T.; Jiang, Y.; Qu, F.; Mayer, A. C.; Parmer, J. E.; McGehee, M. D.; Bao, Z. *Macromolecules* **2008**, *41* (19), 6977–6980.
(17) Dimitrakopoulos, C. D.; Malenfant, P. R. L. *Adv. Mater*. **2002**, *14* (2).
(18) Kelley, T. W.; Boardman, L. D.; Dunbar, T. D.; Muyres, D. V.; Pellerite, M. J.; Smith, T. P. *J. Phys. Chem. B* **2003**, *107* (24), 5877–5881.
(19) Klauk, H.; Halik, M.; Zschieschang, U.; Schmid, G.; Radlik, W.; Weber, W. *Appl. Phys. Lett*. **2002**, *92*, 5259.
(20) Yang, H.; Shin, T. J.; Ling, M.-M.; Cho, K.; Ryu, C. Y.; Bao, Z. *J. Am. Chem. Soc*. **2005**, *127* (33), 11542–11543.
(21) Payne, M. M.; Parkin, S. R.; Anthony, J. E.; Kuo, C.-C.; Jackson, T. N. *J. Am. Chem. Soc*. **2005**, *127*, 4986–4987.
(22) Ito, Y.; Virkar, A. A.; Mannsfeld, S.; Oh, J. H.; Toney, M.; Locklin, J.; Bao, Z. *J. Am. Chem. Soc*. **2009**, *131* (26), 9396–9404.
(23) Yoo, S.; Domercq, B.; Kippelen, B. *Appl. Phys. Lett*. **2004**, *85*, 5427–5429.
(24) Pandey, A. K.; Nunzi, J.-M. *Appl. Phys. Lett*. **2006**, *89* (21), 213506–3.
(25) Sharma, A.; Haldi, A.; W., J. P., Jr.; Hotchkiss, P. J.; Marder, S. R.; Kippelen, B. *J. Mater. Chem*. **2009**, *19*, 5298–5302.
(26) Laquindanum, J. G.; Katz, H. E.; Lovinger, A. J. *J. Am. Chem. Soc*. **1998**, *120* (4), 664–672.
(27) Payne, M. M.; Odom, S. A.; Parkin, S. R.; Anthony, J. E. *Org. Lett*. **2004**, *6* (19), 3325–3328.
(28) Lloyd, M. T.; Mayer, A. C.; Subramanian, S.; Mourey, D. A.; Herman, D. J.; Bapat, A. V.; Anthony, J. E.; Malliaras, G. G. *J. Am. Chem. Soc*. **2007**, *129* (29), 9144–9149.
(29) Zhu, Z.; Waller, D.; Gaudiana, R.; Morana, M.; Muhlbacher, D.; Scharber, M.; Brabec, C. *Macromolecules* **2007**, *40* (6), 1981–1986.
(30) Bechgaard, K.; Krebs, F. C. *Macromolecules* **2005**, *38* (3), 658–659.
(31) Miller, G. P.; Briggs, J.; Mack, J.; Lord, P. A.; Olmstead, M. M.; Balch, A. L. *Org. Lett*. **2003**, *5* (22), 4199–4202.
(32) Murata, Y.; Kato, N.; Fujiwara, K.; Komatsu, K. *J. Org. Chem*. **1999**, *64* (10), 3483–3488.
(33) Li, Z.; Parkin, S. R.; Anthony, J. E.; Lee, S.; Loo, L. *PMSE Prepr*. **2009**, *101*, 1534.
(34) Reese, C.; Bao, Z. *J. Appl. Phys*. **2009**, *105*.
(35) Zhang, W.; Smith, J.; Hamilton, R.; Heeney, M.; Kirkpatrick, J.; Song, K.; Watkins, S. E.; Anthopoulos, T.; McCulloch, I. *J. Am. Chem. Soc*. **2009**, *131* (31), 10814–10815.
(36) Horie, M.; Luo, Y.; Morrison, J. J.; Majewski, L. A.; Song, A.; Saunders, B. R.; Turner, M. L. *J. Mater. Chem*. **2008**, *18*, 5230–5236.
(37) Coffin, R. C.; Peet, J.; Rogers, J.; Bazan, G. C. *Nature Chem*. **2009**, *1*.
(38) Lee, J. K.; Ma, W. L.; Brabec, C. J.; Yuen, J.; Moon, J. S.; Kim, J. Y.; Lee, K.; Bazan, G. C.; Heeger, A. J. *J. Am. Chem. Soc*. **2008**, *130* (11), 3619–3623.
(39) Muhlbacher, D.; Scharber, M.; Morana, M.; Zhu, Z.; Waller, D.; Gaudiana, R.; Brabec, C. *Adv. Mater*. **2006**, *18* (21), 2884–2889.
(40) Mayer, A. C.; Toney, M. F.; Scully, S. R.; Rivnay, J.; Brabec, C. J.; Scharber, M.; Koppe, M.; Heeney, M.; McCulloch, I.; McGehee, M. D. *Adv. Funct. Mater*. **2009**, *19*, 1173–1179.